ACTA MECHANICA SINICA (English Series), Vol.17, No.1, February 2001 ISSN 0567-7718
The Chinese Society of Theoretical and Applied Mechanics
Chinese Journal of Mechanics Press, Beijing, China
Allerton Press, INC., New York, U.S.A.

WAVE-SOIL-PIPE COUPLING EFFECT ON SUBMARINE PIPELINE ON-BOTTOM STABILITY*

Gu Xiaoyun (顾小芸) Gao Fuping (高福平) Pu Qun (浦 群)
(*Institute of Mechanics, Chinese Academy of Sciences, Beijing* 100080, *China*)

ABSTRACT: Wave-soil-pipe coupling effect on the untrenched pipeline stability on sands is for the first time investigated experimentally. Tests are conducted in the U-shaped water tunnel, which generates an oscillatory flow, simulating the water particle movements with periodically changing direction under the wave action. Characteristic times and phases during the instability process are revealed. Linear relationship between Froude number and non-dimensional pipe weight is obtained. Effects of initial embedment and loading history are observed. Test results between the wave-soil-pipe interaction and pipe-soil interaction under cyclic mechanical loading are compared. The mechanism is briefly discussed. For applying in the practical design, more extensive and systematic investigations are needed.

KEY WORDS: submarine pipeline, on-bottom stability, wave-soil-pipe coupling effect, sandy seabed

1 INTRODUCTION

Lateral stability of submarine pipelines requires the balances between the hydrodynamic forces, pipe weight and seabed resistance, as shown in Fig.1. If the sea bottom can not provide enough lateral resistance to balance the horizontal component of the hydrodynamic force, the pipeline breakout will take place, i.e. instability occurs.

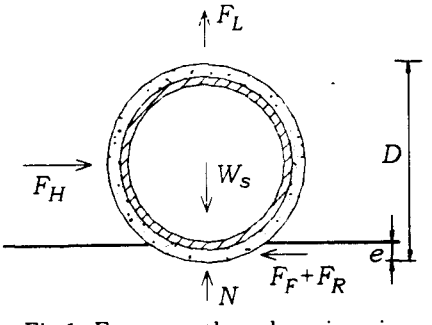

Fig.1 Forces on the submarine pipe

The on-bottom stability experiments on the untrenched pipes by the cyclic loading in the 1980's[1~5] have shown that the traditional design method, in which the soil resistance is estimated by the Coulomb friction, is too conservative. The soil resistance should include a soil passive resistance component as follows

$$F_H = F_F + F_R \tag{1}$$

where F_H is total lateral soil resistance, F_F sliding resistance and F_R lateral passive soil resistance. Due to the increase of lateral resistance, the designed pipe weight can be reduced,

Received 8 June 2000, revised 12 December 2000
* The project supported by the National Natural Science Foundation of China (19772057,19772065) and by the Chinese Academy of Sciences (KZ951-A1-405-01)

thus remarkable cost benefits can be obtained. The above experimental results are reflected in the Veritec's and AGA's design guidelines[4,6]. However, in the above experiments the cyclic loading simulating the wave loading is provided by actuators, so it differs from the real hydrodynamic force. In reality, the hydrodynamic force acts on both the pipe and seabed, and the seabed response to the hydrodynamic force can affect the pipe too. Therefore , precisely speaking, the on-bottom stability of the submarine pipeline concerns the interaction between wave, soil and pipe, but not the pipe/soil interaction under cyclic loading as mentioned in the above references.

Regarding the interaction between flow, pipe and sand bottom, many investigations have been conducted to study scour under pipelines[7~11]. Since the object of those studies is to investigate the scour hole and define the maximum scour depth, most test pipes have been put in the fixed condition. Among them Stansby[11] is an exception. His pipe is free to move vertically, but not horizontally, so the tests do not reflect the phenomena of on-bottom stability either. Foda[12] has studied the breakout of half-buried pipe under hydrodynamic force. According to Chiew[9], when the ratio of pipe embedment e to pipe diameter D reaches 0.5~0.7, there is no scour depth. Indeed, in Foda's tests no scour is observed. Therefore, from the point of flow-soil-pipe interaction, the breakout of untrenched pipes is more complicated than that of half-buried ones.

The object of this paper is to study experimentally the wave-induced instability process of the untrenched submarine pipes, to reveal the differences between the action of hydrodynamic force and that of cyclic loading provided by actuators, and to understand the wave-soil-pipe coupling effect on the on-bottom stability.

It should be mentioned , in case of soft seabed , some embedment inevitably takes place during the pipe laying process, i.e. $e > 0$, as shown in Fig.1, but the value of e/D is very small.

2 TEST FACILITIES AND METHODS

Under the wave action, the water particles oscillate periodically with certain velocities. For simulating the oscillating movement of water particles in the horizontal direction, tests are conducted in the U-shaped oscillatory flow water tunnel, as shown in Fig.2. The water tunnel is made of plexiglass with section area of 0.2 m×0.2 m. By using an air blower with a butterfly-valve, which periodically opens and closes the top of a limb of the water tunnel, the water accomplishes a simple harmonic oscillation

$$A = A_0 \sin \omega t \tag{2}$$

where $\omega = 2\pi/T$, A_0 is amplitude of the oscillating flow, ω cyclic frequency and T period of the oscillating flow, which equals 2.6 s. The amplitude can be varied continuously within 5~200 mm. Thus the maximum water particle velocity of the oscillating flow U_m is

$$U_m = \omega A_0 \tag{3}$$

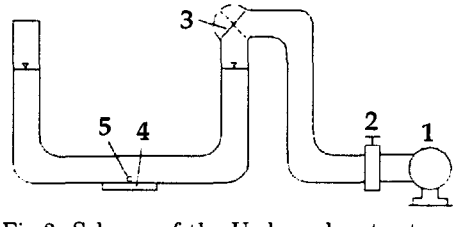

Fig.2 Scheme of the U-shaped water tunnel
1 air blower, 2 regulating valve
3 butterfly-valve, 4 soil box
5 test pipe

The water level change is recorded by using a water pressure transducer and data acquisition system.

The lower part of the water tunnel is the test section, under which a soil box of 0.6 m long, 0.2m in width and 0.035 m in depth is constructed. The soil box is filled with sand, which is regarded as sand bed at the sea bottom. The test pipe is laid directly on the soil surface. Due to the pipe weight and the operation reason, some initial embedment always exists, although the amount of embedment is very small. Conventionally, $e/D = 0.03 \sim 0.05$.

The pipes are composed of aluminium, with length of 0.19 m, so that a distance remains between the pipe end and the side wall of the water tunnel. The pipes are divided into three groups with different diameters: 1.4. 2 and 3 cm. In each group pipes have different weights.

During the test the amplitude of the oscillatory flow is controlled to simulate the history of wave loading, and the instability process of the pipe is observed and recorded by the video camera.

The sand beds consist of medium sand and fine sand, the grain size distribution curves of which are shown in Fig.3. The moist sand is first saturated, then packed in the soil box under water, and finally trimmed with a scraper. The index properties of the sands are shown in Table 1. The difference of the unit weights for different tests are controlled within the error of 5 ‰.

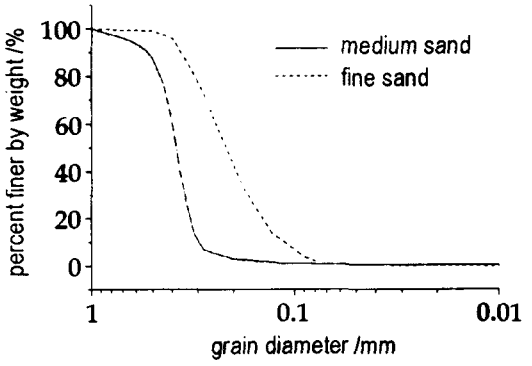

Fig.3 Grain size distribution curves

Table 1 Index properties of the test sands

Mean grain size	Grain size at which 10% of the soil weight is finer	Uniformity coefficient	Unit weight	Dry unit weight	Initial void ratio	Relative density
d_{50}	d_{10}	Cu	$\gamma(\mathrm{kN/m^3})$	$\gamma_d(\mathrm{kN/m^3})$	e_0	D_r
0.38	0.30	1.4	19.00	14.80	0.73	0.37
0.21	0.11	2.0	21.05	17.47	0.56	0.60

3 NON-DIMENSIONAL PARAMETERS

Non-dimensional parameters related to the flow around the pipe are as follows[13,14]: Reynolds number Re, the ratio of inertia force to viscous force

$$Re = \frac{U_m D}{\nu} \tag{4}$$

Froude number Fr, the ratio of inertia force to gravity force, which reflects the dynamic similarity of flow with gravity forces acting, as follows

$$Fr = \frac{U_m}{\sqrt{gD}} \tag{5}$$

Keulegan-Carpenter number KC, non-dimensional parameter related to the hydrodynamic force on the pipe under wave action

$$KC = \frac{U_m T}{D} \tag{6}$$

where ν is viscosity and g is gravity acceleration.

Sandy bottom is distributed in many areas in South China Sea, where Fr and KC change between 0~0.5 and 0~20, respectively. In our test condition, Fr and KC are in these ranges, but Re is smaller than the actual condition by two orders.

Since the study of wave/soil/pipe interaction directly affects the designed pipe weight, the non- dimensional parameter of pipe weight is introduced

$$G = \frac{W_s}{\gamma' D^2} \tag{7}$$

where W_s represent submerged weight of pipe per unit length and γ' is buoyant unit weight of soil.

4 EXPERIMENTAL RESULTS

4.1 Phenomena of Instability Process

4.1.1 Characteristic times

When the amplitude of oscillatory flow A_0 increases with a constant velocity, the following characteristic times can be identified: (see Fig.4)

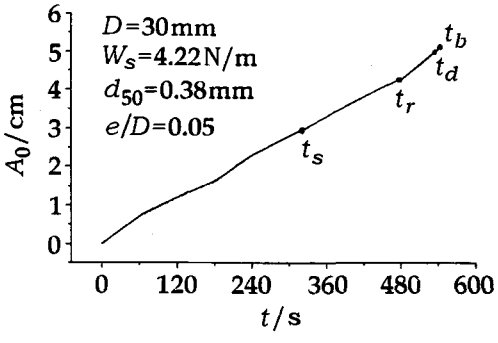

Fig.4 Characteristic times

$t = t_s$: Within a distance apart from the pipe, the sand grains at the bed surface start to move visibly. Onset of scour occurs.

$t = t_r$: The pipe rocks slightly.

$t = t_d$: The pipe detaches itself from the sand bed.

$t = t_b$: The pipe rolls away, or breakout occurs.

Since the submarine pipelines can not roll in reality, t_d is assumed to be the time for losing stability.

4.1.2 Phases of pipe instability process

With the increase of A_0, the pipe and the surrounding sand bed experience the following phases:

(1) Totally stable phase ($t < t_s$) (see Fig.5(a))

(2) Metastable phase ($t_s < t < t_r$)

When the flow velocity is large enough to create considerable amount of sediment in suspension, it makes the main contribution to the sediment transport and piles up in the outer directions. While in the vicinity of the pipe, pits are gradually formed on both sides. (See Fig.5(b)) In this phase the length of the contact between the pipe and seabed Δx increases.

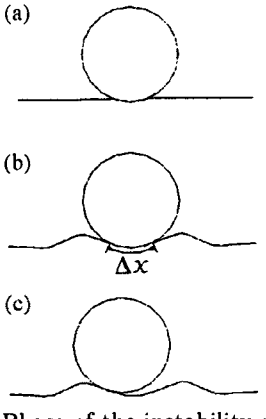

Fig.5 Phase of the instability process

(3) Pre-failure phase ($t_r < t < t_d$)

At $t = t_r$, the pipe begins to rock slightly. Δx decreases gradually with the increase of erosion, till $t = t_d$, when the pipe detaches itself from the sand bed (see Fig.5(c)).

(4) Breakout phase ($t_d < t < t_b$)

At $t = t_b$, the pipe suddenly rolls out, or breakout takes place. In most cases in our tests, t_b occurs just after t_d, i.e. t_b almost coincides with t_d, and the breakout phase is a very short moment. Actually the pipe can not roll, so this phase is excluded in the later data reduction.

4.1.3 Instability process for pipes with different weight

Figure 6 shows the instability process of pipes with different submerged weight. Most of the pipes possess all the above stated characteristic times and phases, but there are few exceptions. For the lightest two pipes with diameter of 3 cm, the submerged weight W_s of 1.52 N/m and 1.61 N/m on medium and fine sand, respectively, breakout or pipe rolling occurs at $A_0 < A_s$. The sand grain movement has not been observed, the metastable and pre-failure phases are also missing. Pipe rolling should not take place in reality, so these two cases should be excluded in the data reduction.

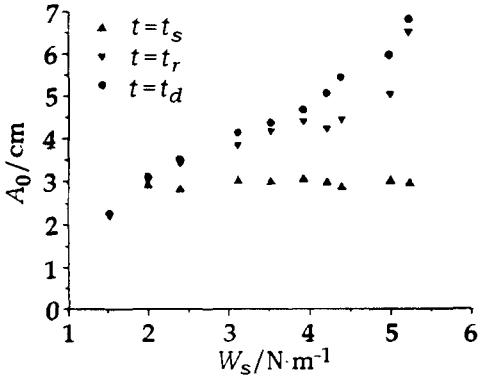

Fig.6 Instability process for pipes with different weight ($D = 3$ cm)

For the heavy pipes of $d = 3$ cm with G over 0.6 and 0.5 (these G will be denoted as G_u) on medium and fine sand, respectively, there is no t_b. At $t > t_d$, more and more sand sediments pile up at both sides of the pipe, and the pipe stability increases. In other words, for $G > G_u$, t_d can not be considered as the time for losing stability.

Figure 6 also shows that A_s, the oscillatory flow amplitude at $t = t_s$, has the same value for pipes with different weight, as shown in Table 2. It implies that the water particle velocity is the main cause of onset of scour or erosion. At that moment the pipe is stable, and the pipe weight has no effect on erosion.

Table 2 A_s for pipes of $D = 3$ cm with different weights

Soil type	D(cm)	A_s(cm)								$\bar{A}_s$(cm)
medium sand	3.0	2.90	2.81	3.00	2.97	3.03	2.94	2.84	2.98	2.93±0.06
		2.88	2.89	2.92	2.96					
fine sand	3.0	2.70	2.71	2.70	2.68	2.65	2.75	2.75	2.69	2.71±0.04
		2.79								

4.2 Correlation Between Pipe Weight and Hydrodynamic Parameters

As mentioned above, t_d is assumed to be the time for losing stability. Thus the hydrodynamic parameters are calculated from the water particle velocity at t_d.

The correlation between KC number and non-dimensional pipe weight G is shown in Fig.7(a,b) for medium sand and fine sand, respectively. For the same diameter, exists a linear KC-G relationship. For different pipe diameters, the linear KC-G relationships are different. It is shown that in case of using KC number for data reduction, the effect of pipe

diameter is significant. For the same pipe diameter, sands of different particle size possess different KC-G relationships, but the difference is relatively small.

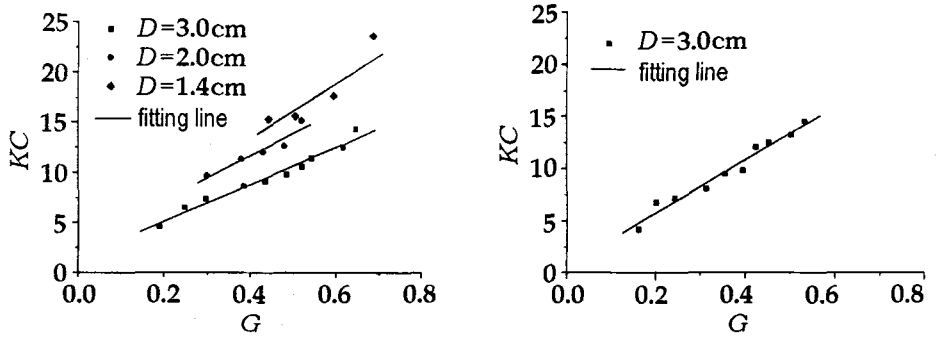

(a) Medium sand (b) Fine sand

Fig.7 KC-G correlation

Figure 8 shows the correlation between Fr and G. For the same sand, all the data with different pipe diameters fall within the range with the same linear relationship. This line can be regarded as the critical line for pipe instability. For sands with different particle size, Fr-G relationships are somewhat different. It matches with Poorooshasb's point[15], that indicates the importance of Fr in case of water-structure-soil interaction.

Table 1 shows that two test sands have different relative density as well as different particle size. The relative density is included in the submerged unit weight, so the additional effect of the particle size should be considered. Since the particle size of sands strongly affects the soil permeability, which is an important factor of water-soil-pipe coupling effect as will be discussed later, and the coefficient of permeability has a well-known correlation with the particle size d_{10}[16], thus the following modified Froude number for the fine sand

$$Fr' = Fr \Big/ \left[\frac{(d_{10})_M}{(d_{10})_F}\right]^{0.2} \tag{8}$$

is introduced. The Fr'-G relationship for fine sand coincides with the Fr-G line for medium sand, as shown in Fig.9. In Eq.(8) the suffix M or F denotes medium sand or fine sand.

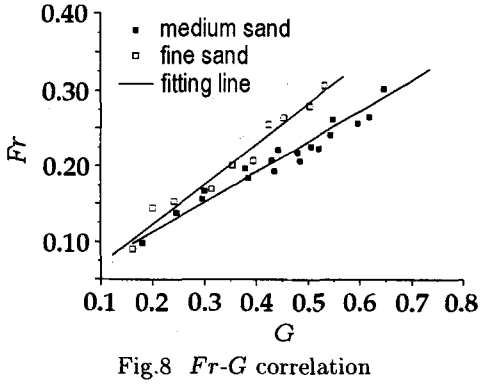

Fig.8 Fr-G correlation

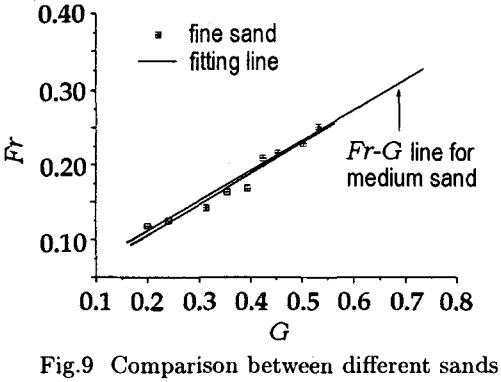

Fig.9 Comparison between different sands

It should be mentioned, that the linear relationship is valid in a limited range. Because the cases when breakout occurs at $A_0 < A_s$ are out of the scope of our study, the lower limit

depends on A_s as follows

$$Fr = 2\pi A_s / T\sqrt{gD} \tag{9}$$

while the upper limit is defined by the non-dimensional pipe weight G_u. For $G > G_u$, Fr-G line will turn upward.

Since the Froude number in our tests is close to that in some real condition, it is convenient to find out the pipe weight for the prototype from the Fr-G correlation. However, it should be mentioned, that the above Fr-G correlation is valid for a limited range of KC value$\leq$20.

4.3 Effect of Initial Pipe Embedment

Palmer et al.[3] has reported that initial pipe embedment increases the lateral resistance. Three different values of initial embedment ($e/D = 0.05, 0.10, 0.15$) have been tested by us with one pipe ($D = 3\,\mathrm{cm}$, $W_s = 4.22\,\mathrm{N/m}$). The results are shown in Table 3. For the smallest e/D, all four characteristic times exist, and breakout occurs just after t_d. The increase of e/D does not affect A_s much, but increases the values of A_r and A_d. For $e/D = 0.1$, although detachment has been observed after the pipe rocking, breakout does not occur due to the piling up of the sediments on both sides of the pipe. For even larger initial embedment, after some time of slight rocking, self-burial occurs. (See Fig.10) Thus the on-bottom stability increases with the increase of initial embedment.

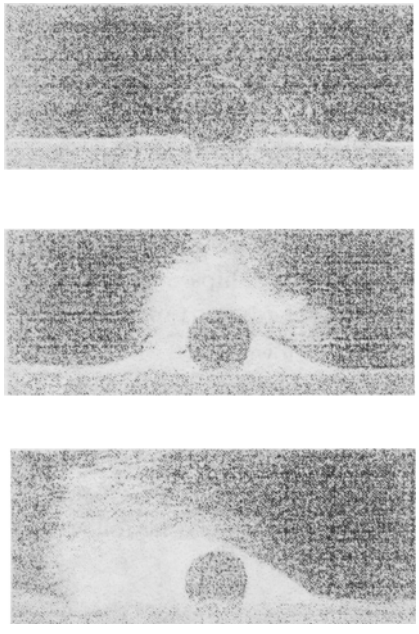

Fig.10 Self-burial of the pipe

Table 3 Results with different initial embedment

e/D	A_s(cm)	A_r(cm)	A_d(cm)	Does breakout occur?
0.05	2.9	4.2	5.0	yes
0.10	2.9	5.3	5.9	no
0.15	3.0	5.7	self-burial	no

4.4 Effect of Loading History

All the above tests are conducted under a same loading history, i.e. the oscillatory flow amplitude increases with a constant velocity $\dot{A}_0$. In order to explore the effect of loading history, different amplitude velocities have been adopted. The results are shown in Table 4.

The velocity of the oscillatory flow amplitude does not affect A_s, but A_r and A_d decrease with the increase of $\dot{A}_0$. For the smallest $\dot{A}_0$, breakout does not occur. It shows that not only the water particle velocity affects the pipe stability, but the loading history also plays an important role in the on-bottom stability.

Table 4 Results with different velocities of flow amplitude

A_0(cm/s)	A_s(cm)	A_r(cm)	A_d(cm)	Does breakout occur?
1.8×10^{-2}	2.89	4.1	4.5	yes
9.0×10^{-3}	2.94	4.2	5.0	yes
4.5×10^{-3}	2.92	4.5	5.1	no

Furthermore, the storm growing is not always continuous, so experiments with 4 types of loading history have been tested. For type (a), the amplitude increases with a constant velocity as stated above. For the other three types, first increase the flow amplitude with constant velocity till a value of A_c, then maintain A_c for 5 minutes, i.e. about 115 cycles, and finally increase the amplitude as before. These three types of loading history give different values of A_c. For (b), $A_c < A_s$. For (c), $A_s < A_c < A_r$. For (d), A_c is just above A_r. The results are shown in Fig.11. When $A_0 = A_c < A_s$, the sand grains at the bed surface have not started moving, so the increase of the flow amplitude after maintaining A_c for 115 cycles has the same effect on pipe stability as for type (a). In Fig.11, A_d at line a and line b are on the same level. When $A_s < A_c < A_r$, at the time of reaching A_c, the sand bed has entered into the metastable phase. During the period of maintaining A_c for 115 cycles, more and more sand grains pile up on both sides of the pipe due to the effect of vortex. The higher sediment piling makes the increase of the pipe stability, so the point of losing stability at line c in Fig.11 is higher than that at line a. For the last type, when A_0 reaches A_c, the pipe has just started rocking. While A_c is maintained, the slightly rocking pipe returns to the static condition due to the sediment piling. Only after the flow amplitude is increased to some higher level, the pipe slightly rocks again. In Fig.11 the point of losing stability at line d is even higher.

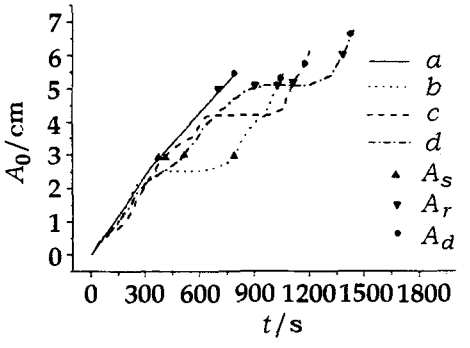

Fig.11 Effect of loading history

It implies that some intermittently growing storm could be beneficial for the pipe stability in spite of the same wave height, and the experimental results with constant amplitude velocity are inclined to the safe side.

5 COMPARISON WITH THE PREVIOUS EXPERIMENTS

Wagner et al.[2] reported that cyclic loading caused pipe penetration into the soil and soil mounding in front of the pipe, therefore resulted in increased lateral soil resistance, which far exceeded those predicted by Coulomb friction. The embedment of the pipe in the sediment is illustrated in Fig.12 (from [4]). The previous experiments also indicated the effect of loading history and initial embedment on the lateral resistance. Our tests (see Fig.5) and the previous tests as shown in Fig.12 have some similarity. On both sides of the pipe soil mounding or piling up of the sediments is investigated. So the same conclusion that the resistance is larger than that predicted by Coulomb friction is reached. Both tests

also explored the effect of loading history and initial embedment. The similarity is very important. It shows that although the previous tests have not included the real hydrodynamic action, the design method based on those tests is correct.

However, the mechanism of the phenomena in different kinds of tests is quite different. The previous experimental results are caused by self-penetration of the pipe under cyclic mechanical loading. While in our tests scour or erosion plays an important role, which reflects the actual submarine condition.

The pipe-soil interaction models obtained by DNV[2] and AGA[4] are largely empirical. For example, in DNV's model, the right terms in Eq.(1) are

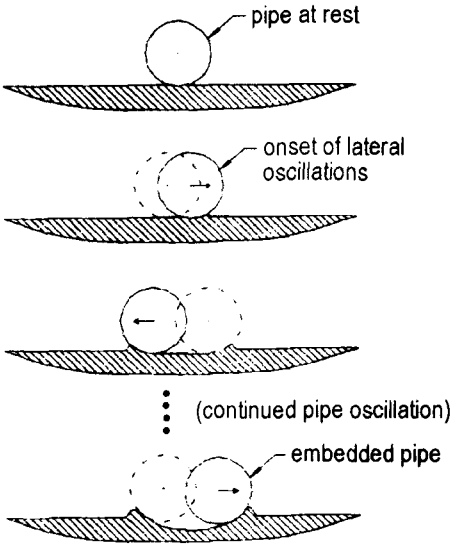

Fig.12 Embedment of pipe in soft sediments (from [4])

$$F_F = \mu(W_s - F_L) \tag{10a}$$

$$F_R = \beta\gamma'\alpha \tag{10b}$$

where μ is coefficient of friction between the pipe and soil, F_L represent hydrodynamic lift force, β is a function of the pipe displacement and the lateral loading history, and α is one half of the area of a vertical cross section of the soil displaced by the pipe during the penetration and oscillations. The parameters β and α are empirical, depending on how the tests are conducted and the repeatability of the tests.

From our wave-soil-pipe interaction tests, the Fr-G relationship demonstrates the relationships between water particle velocity, soil properties, pipe diameter and submerged weight of the pipe. All the parameters involved have obvious physical meaning. Because of the limited test data, the final model has not been obtained yet, but the Fr-G relationship implies that it can serve as a supplementary analysis tool for the design.

It should be mentioned, in the present paper, that the pipe is not constrained against rolling, which is different from the previous tests. In reality, the pipe can not roll, but it is not fully constrained either. From our point, during the pipe testing described in 4.1.2, except the breakout phase, all the other three phases do reflect the actual submarine condition.

6 DISCUSSION ON THE MECHANISM

The experimental results show that the scour is an important phenomenon during the pipe instability process and also an indication of wave-soil-pipe coupling effect. According to Mao[10] and Chiew[9], the onset of scour is due to the combined action of the vortexes and underflow or piping effect.

Truly, above the soil surface the sand grains start to move visibly due to the vortexes at $t = t_s$. Since the smaller are the sand particles, the easier they are to be carried away, so the value of A_s for fine sand is smaller than that for the medium sand, as shown in Table 2.

The vortexes also play the role in the sediment piling, which is shown in Fig.10.

While under the sea bottom the water flows through the soil, and the flowing water exerts upon the soil particles a seepage force. Permeability, as a property of a porous material which permits the seepage of water through its interconnecting voids, should be considered as an important factor.

The magnitude of the seepage force F_s is a function of the prevailing hydraulic gradient

$$F_s = \gamma_w i \tag{11}$$

where $i = \Delta p/\Delta x$ is the hydraulic gradient, Δp is the pressure difference between the entrance and exit of the flow channel and Δx is length of the contact between the pipe and soil. As Δp increases faster than Δx or Δx decreases, i increases. When the hydraulic gradient exceeds its critical value i_c, hydraulic instability occurs. At that moment soil particles just beneath the pipe are loosened, and the pipe embeds to the lower level.

For sands, i_c is expressed as[17]

$$i_c = (G_s - 1)(1 - n) \tag{12}$$

where G_s is specific gravity and n is porosity. For both test sands, i_c is close to unity. By using Hazen's formula[16]

$$k = 100\, d_{10}^2 \tag{13}$$

where k is coefficient of permeability, the estimated permeability coefficient of the fine sand is smaller than that of the medium sand by one order. According to the Darcy's law

$$u = ki \tag{14}$$

the velocity of the flow u at i_c through the fine sand is smaller, so it is easier to have the pipe embedment in the fine sand. The embedment is a favourable factor for pipe stability. It explains why the Fr-G line for fine sand is above that for medium sand. The reason why we use d_{10} to obtain the modified Froude number (see Eq.(8)) is just to consider the effect of permeability.

In order to understand the mechanism thoroughly, measurements of the pipe movements, hydrodynamic pressure around the pipe and the pore water pressure beneath the pipe will be conducted further.

7 CONCLUSIONS

(1) The wave-soil-pipe coupling effect upon the untrenched submarine pipeline stability on sands is for the first time investigated experimentally. Tests are conducted in the U-shaped oscillatory flow water tunnel.

(2) During the pipe instability process the characteristic times t_s, t_r, t_d and t_b are revealed, and different phases are identified. The water particle velocity is the main cause for starting sand particle movements. t_d is considered as the time for losing stability.

(3) By the non-dimensional analysis the correlations between the pipe weight and hydrodynamic parameters have been obtained. The linear relationship between Froude number and non-dimensional pipe weight can be used as a supplementary analysis tool for practical design.

(4) The tests show that factors, such as initial pipe embedment and loading history, affect the pipeline stability.

(5) Test results between the wave-soil-pipe interaction and pipe-soil interaction under cyclic mechanical loading are compared. The phenomena are similar, but the mechanism is quite different.

(6) The mechanism is briefly discussed. Scour, as an indication of wave-soil-pipe coupling effect, is a result of combined action of vortexes above the seabed and seepage under the sea bottom. Thus permeability is an important factor, whose effect is included in d_{10}, the diameter for relating particle size and permeability.

(7) In order to understand the mechanism thoroughly and to reflect the wave-soil-pipe coupling effect in the practical design, more extensive and systematic investigations are needed.

REFERENCES

1 Brennodden H, Sveggen O, Wagner DA, Murff JD. Full-scale pipe-soil interaction tests. OTC paper 5338, 1986

2 Wagner DA, Murff JD, Brennodden H, Sveggen O. Pipe-soil interaction model. OTC paper 5504, 1987

3 Palmer AC, Steenfelt JS, Steensen-Bach JO, Jacobsen V. Lateral resistance of marine pipelines on sand. OTC paper 5853, 1988

4 Allen DW, Lammert WF, Hale JR, Jacobsen V. Submarine pipeline on-bottom stability: recent AGA research. OTC paper 6055, 1989

5 Brennodden H, Lieng JT, Sotberg T, Verley RLP. An energy-based pipe-soil interaction model. OTC paper 6057, 1989

6 Det norske Veritas. On-bottom stability design of submarine pipelines. Recommended Practice E305, 1988

7 Sumer BM, Fredsoe J. Onset of scour below a pipeline exposed to waves. *Int J Offshore and Polar Engng*, 1991, 1: 189~194

8 Pu Qun, Li Kun. Scour of the sand bed below the pipeline in oscillating flow. *Acta Mechanica Sinica*, 1999, 31: 677~681 (in Chinese)

9 Chiew YM. Mechanics of local scour around submarine pipelines. *J Hydraulic Engng*, 1990, 116: 515~529

10 Mao Y. Seabed scour under pipelines. In: Proceedings of 7th International Symposium on Offshore Mechanics and Arctic Engineering (OMAE), Houston, 1988. 33~38

11 Stansby PK, Starr P. On a horizontal cylinder resting on a sand bed under waves and currents. *Int J Offshore and Polar Engng*, 1992, 2: 262~266

12 Foda MA, Chang J, Law A. Wave-induced breakout of half-buried marine pipes. *J Waterway, Port, Coastal and Ocean Engng*, 1990, 116: 267~286

13 Massey BS. Mechanics of fluids, 5th ed. UK: Van Nostrand Reinhold Co. Ltd, 1983

14 Herbich JB. Hydromechanics of submarine pipelines: design problems. *Can J Civil Engng*, 1985, 12: 863~874

15 Poorooshasb F. On centrifuge use for ocean research. *Marine Geotechnology*, 1990, 9: 141~158

16 Lambe TW, Whitman RV. Soil mechanics, SI Version. New York: John Wiley & Sons, 1979

17 Jumikis AR. Soil mechanics. Princeton: Van Nostrand, 1962